PROCEEDINGS OF SCIENCE

Tests and calibration of detector strings for the KM3NeT/ARCA neutrino telescope

S. Mastroianni,[a,*] F. Badaracco,[b] F. Benfenati Gualandi,[c] G. Ferrara,[d,e] V. Kulikovskiy,[b] W. Idrissi Ibnsalih,[a] D. Paesani,[c] P. Piattelli,[c] G. Riccobene[c] and S. Sanfilippo[c] for the KM3NeT Collaboration

[a] *INFN, Sezione di Napoli, Complesso Universitario di Monte S. Angelo, Via Cintia ed. G, Napoli, 80126, Italy*

[b] *INFN, Sezione di Genova, Via Dodecaneso 33, Genova, 16146, Italy*

[c] *INFN, Sezione di Bologna, Viale Berti-Pichat 6/2, 40127 Bologna, Italy*

[d] *INFN, Laboratori Nazionali del Sud, (LNS) Via S. Sofia 62, Catania, 95123, Italy*

[e] *Università di Catania, Dipartimento di Fisica e Astronomia "Ettore Majorana", Via Santa Sofia 64, Catania, 95123 Italy*

E-mail: stefano.mastroianni@na.infn.it

KM3NeT is a network of underwater Cherenkov neutrino telescopes currently under construction at two sites in the Mediterranean Sea. ARCA, located offshore the Sicilian Coast (Italy), is optimized for the detection of high energy cosmic neutrinos, while ORCA situated off the coast of Toulon (France), is designed for studying atmospheric neutrinos. Both detectors consist of vertical string-like detection units, each comprising 18 optical modules. Each optical module houses 31 3-inch photomultiplier tubes and electronics for control and power supply, an acoustic sensor, tiltmeter-compasses and readout and data transmission. The data are acquired according to a triggerless streaming readout scheme, where the optical modules act as underwater nodes transmitting all data and communicating with the control station on shore via a network of optical fibers. To optimise event direction reconstruction, the optical modules are synchronized to O(∼ 1) ns accuracy using the White Rabbit time synchronization protocol, while their locations underwater are known with accuracy O(∼20) cm at any time using a custom acoustic positioning system. Following the first phase of construction, which relied on a KM3NeT *customized* version of the White Rabbit protocol, a new network architecture following the *standard* White Rabbit protocol has been implemented to improve the maintainability and scalability of the system.

In this contribution the setup, procedure and protocols adopted to test the ARCA detection units under standard White Rabbit configuration is described. Specifically, the system of instrumentation for optical, acoustic and data readout systems and calibration measurements in the final stage of integration of a detection unit are presented. With this system the detection units are validated under operating conditions prior to their installation at the sea bed.

39th International Cosmic Ray Conference (ICRC2025)
15–24 July 2025
Geneva, Switzerland

*Speaker

© Copyright owned by the author(s) under the terms of the Creative Commons Attribution-NonCommercial-NoDerivatives 4.0 International License (CC BY-NC-ND 4.0).

PoS(ICRC2025)1116

1. Introduction

The neutrino telescope KM3NeT[1] is a deep sea infrastructure with detectors under construction at two sites in the Mediterranean Sea. The ORCA (Oscillations Research with Cosmics in the Abyss) detector is located about 40 km off-shore Toulon, France at 2.5 km depth. It is designed for low energy studies from a few hundreds of MeV to sub-TeV. The ARCA (Astroparticle Research with Cosmics in the Abyss), located about 100 km off-shore Capo Passero, Sicily, Italy at a depth of 3.5 km, is dedicated to high-energy studies (up to a few hundred PeV).
Although the scientific goals of the detectors are different, they are built with the same technology, based on mulit-PMT Digital Optical Modules (DOMs), pressure resistant glass spheres containing 31 photomultipliers (PMT), a number of calibration devices, and read-out electronics[2].
The DOMs measure the Cherenkov light induced in seawater by secondary charged particles produced by interactions of neutrinos inside or nearby the detector volume. The trajectories of the charged particles through the detectors are reconstructed by combining an accurate measurement of the time of arrival of the photons and the position of the optical modules. All elements of the telescope need to be calibrated in time at nanosecond level accuracy and in position with an accuracy of about 10 cm, to reach the required angular resolution of about 0.1° at 100 TeV for ARCA[1].
The calibration tests performed at Detection Units (DUs) at the ARCA DU integration laboratories are described. Recent upgrades of the data acquisition architecture are briefly described in Sec. 2, focusing on the calibration procedures. A description of the calibration setups and processes are presented together with the most significant results in Sec. 3.

2. The Detection Unit

A detection unit comprises 18 DOMs connected through a backbone cable to a base module (BM) and then to a junction box. The submarine network of junction boxes is connected to a control station on the shore via a long electro-optical cable.
The DOMs in the ARCA (ORCA) array are distributed in the seawater volume with an average horizontal distance of about 90 (20) m and a vertical distance of about 36 (9) m, with the lowest modules at about 70 (30) m above the seabed. The targeted instrumented volume of KM3NeT is more than 1 km^3. In fact, the goal is to install in total 115 DUs for ORCA and 230 DUs for ARCA within the next few years. The data acquisition (DAQ) system of KM3NeT has been designed in order to guarantee the sub-nanosecond time synchronization between the DOMs by means of the White Rabbit (WR)[4] technology. This is implemented in two different designs: a "broadcast" system[3], which has been used in the first phase of the construction of ARCA and ORCA, and a standard WR system, which is now used for current DU production.
The "broadcast" architecture consists of one link used to broadcast slow-control commands to DOMs and BMs and one direct uplink for the central logic boards (CLBs) in each DOM back to the on-shore station. This asymmetry does not allow for exploiting a standard WR ethernet technology and the firmwares of the WR nodes (for both shore station and off-shore nodes) have been customized.
The new architecture is based on a new aggregation layer implemented directly in the DUs. The

PoS(ICRC2025)1116

DOMs have been upgraded in order to implement a WR-slave node by using standard WR firmware. The new design enables taking advantage of the official WR developments and maintenance and allows for the use of fewer cable connections to the sea infrastructure. This upgrade has required a redesign of the BM. Basically, it hosts two standard core board switches (labeled Wet-WR Switches WWRS-A and WWRS-B), each with 18 transceivers. Thus, the two switches are connected to 18 DOMs providing 12 cold redundancies.
The construction and integration of DUs involve several steps that take place at different laboratories of the KM3NeT Collaboration[5]. At the DU integration site, the DOMs, including its calibration devices and already tested for performance, are electrically and optically connected to the vertical electro-optical data cable (VEOC). Then, the BM, integrated and enclosed in a titanium container, is connected to the VEOC. The resulting DU can be attached to the other auxiliary devices, namely hydrophone and eventually an acoustic transmitter (beacon). The entire DU, placed in a dark box and connected to a test-station, can be put for the first time into operation and each component is tested under close to real conditions before its final commissioning.

3. Test and calibration in dark box

At the shore-station, as shown in Fig. 1, based on standard WR switches (labeled Dry-WRS), the detector interface for both control and data readout is managed. The Control Unit (CU), a software component running in the shore-station, is used for detector control and user interface to the central KM3NeT data base. Trigger and Data Acquisition System (TriDAS) software components process the optical and acoustics data streams coming from the DU. All the calibration steps rely on a central data base, where the detector information is stored, along with running parameter sets ("runsetups") and calibration information. The detector definition, the operating and logging parameters such as temperature and humidity in the DOMs, compass and tilt meter values, current, strength of the communication link, can be retrieved by the CU. Then, a fast analysis and online monitoring can be performed on a subset of the selected data showing the status of the data taking (PMT and trigger rate, calibration checks, etc.).

3.1 Setup and configuration

After the CU configurations, the communication with the BM and DOM nodes can be established. Then, the first set of runsetups can be created and used for calibration and later for science operation and data taking. In fact, with the first runs the DAQ and communication are tested in order to swiftly identify potential malfunctioning.
After about one day of darkening, PMTs are operated at high voltage as recommended by the vendor and the dark count rates are monitored. Channels with unusual behavior are further investigated and eventually excluded. Typically, a PMT is excluded when its counting rates are extremely low or high, i.e., <100 Hz or >10 kHz, respectively.

3.2 Power measurements

After the first successful data taking runs, the DU electrical tests and power consumption measurements can be performed according to a well-defined sequence of operating conditions of CLB status (in both BM and DOMs) and the attached devices to the BM. Because the new

PoS(ICRC2025)1116

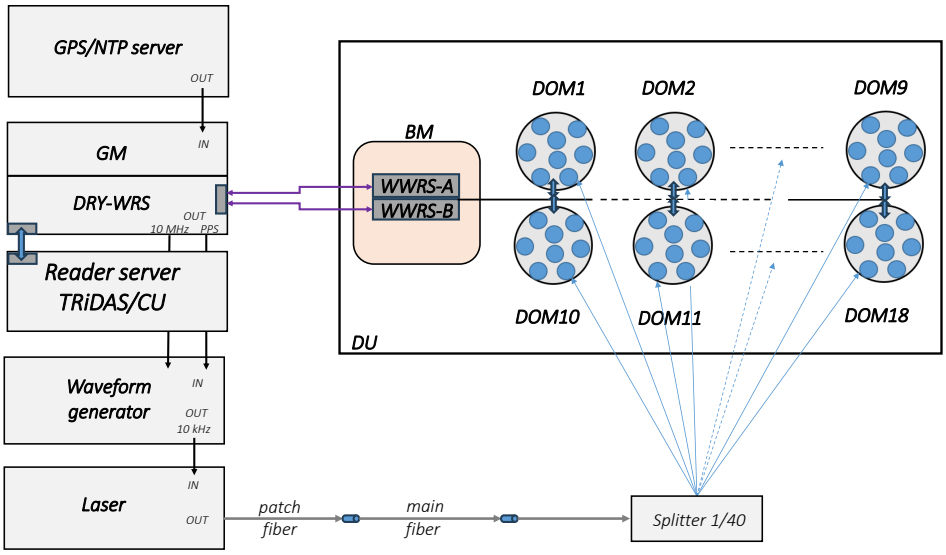

Figure 1: Setup for DU test and calibration during the time measurements.

WR architecture has a higher power consumption (224 mA at 363V) compared to the previous architecture (41 mA at 375 V), a cooling system is required for the BM vessel during the duration of tests. A continuous monitor of the temperatures of the critical devices (FPGA, glenair transceivers etc..) is also implemented.
The first measurements are carried out with only the BM turned on and then by turning on the acoustic beacon (if present) and then the hydrophone. The next step is the power measurements when the power board distributes the 363 V to the VEOC. In the final step all DOMs are switched on and running. Current measurements are carried out by a microcontroller hosted in the BM CLB that reads the sensors.
These measurements allow KM3NeT to verify that everything is working well but also to have reference values for the detector deployment.

3.3 HV tuning

In order to achieve a proper PMT operating mode, PMT gains must be equalized using the HV tuning procedure. The HV tuning, which is defined by a desired gain of 3×10^6, uses the gains resulting from a fit to the time over threshold (ToT) distribution[6]. For each PMT of a DOM, all hits detected during a given run are read. The tuning procedure can be accomplished with a HV scan spanning the interval between -56V and 56V in steps of 8V centered around the vendor nominal value whereby a few minutes of data for each HV are sufficient. By fitting multiple single photoelectron ToT distributions taken at different high voltage settings as a function of the PMT gain, the HV value that gives rise to a nominal gain can be estimated. The final HV tuned value can be evaluated from a linear behaviour of PMT gain versus HV.

3.4 Checks on acoustic and compass data

The acoustic positioning system relies on two subsystems: acoustic receivers installed on the DU elements (hydrophone near the BM and the piezoelectric devices glued the glass sphere in

PoS(ICRC2025)1116

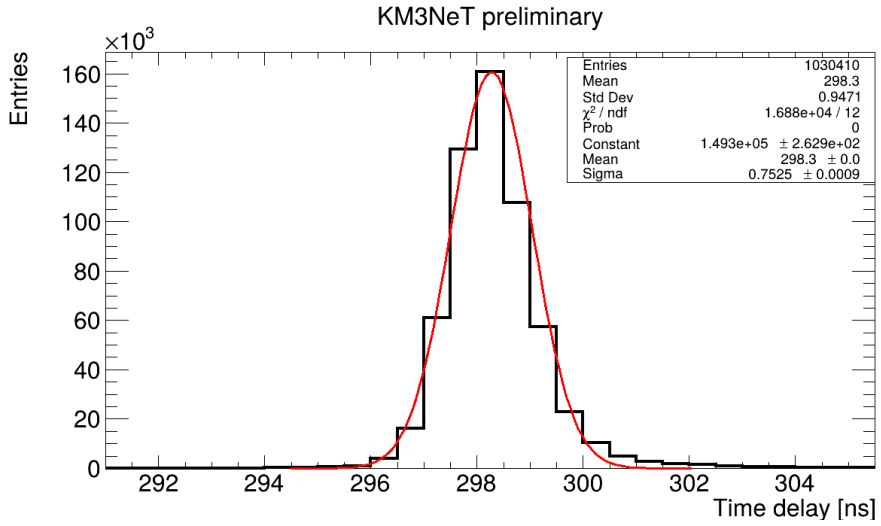

Figure 2: Arrival time distribution of first hits of a PMT. The time offset is calculated by the mean value of the Gaussian fit.

each DOM) and acoustic transmitters with georeferenced positions at the sea bed[7]. In addition to the communication tests and power measurements of the BM acoustic devices (Sec. 3.2), several functional tests of all the acoustic receivers are performed by using a waveform generator and a sound amplifier-and-splitter (1/20). A sinusoidal wave emission at 30-kHz frequency and an amplitude of 2 Vpp is set. The acoustic emission is synchronized with the WR system, and the generation is triggered by the pulse per second (PPS) signal. The acoustic data, consisting of the digitized wave-forms, are routed to the Acoustic DataFilter processes that reconstruct the detection-time, also referred to as time of arrival (ToA). The correct detection of acoustic signals is checked through an analysis of the ToA of the emitters signals and their synchronicity with respect to the WR clock.
During data taking each CLB sends to the test-station raw accelerometer and magnetometer data. Then, a dedicated software tool converts these raw values into actual readings. A simple data filtering for proper data transfer is performed here without any check on the data quality.

3.5 Timing measurements in dark box

The sub-nanosecond time synchronization among the DOMs is an important goal of the DU timing calibration. While the PMT intrinsic offsets are due to different transit times (TTs) about ±2 ns between different PMTs, time offsets of the DOMs are dominated by the electronics readout line and the clock signal distribution from shore station to the off-shore nodes. In fact, the new WWRS architecture provides the full synchronization between the test-station and the DOMs. Nevertheless, some residual electro-optical asymmetries, delays and configuration parameters can introduce small systematic offsets that will be measured and accounted for during the calibration phase. Further details regarding the optical network and WWRS calibration scheme can be found [8].
The goal is to determine the relative time offsets between the different DOMs performed in the dark box by means of a laser source and a light distribution system that provides laser pulses at s.p.e. level directly and simultaneously to two reference PMTs of each DOM. In Fig. 1 the setup of the DU time calibration is shown. The Grand Master (GM) and DRY-WR switches, synchronized to

PoS(ICRC2025)1116

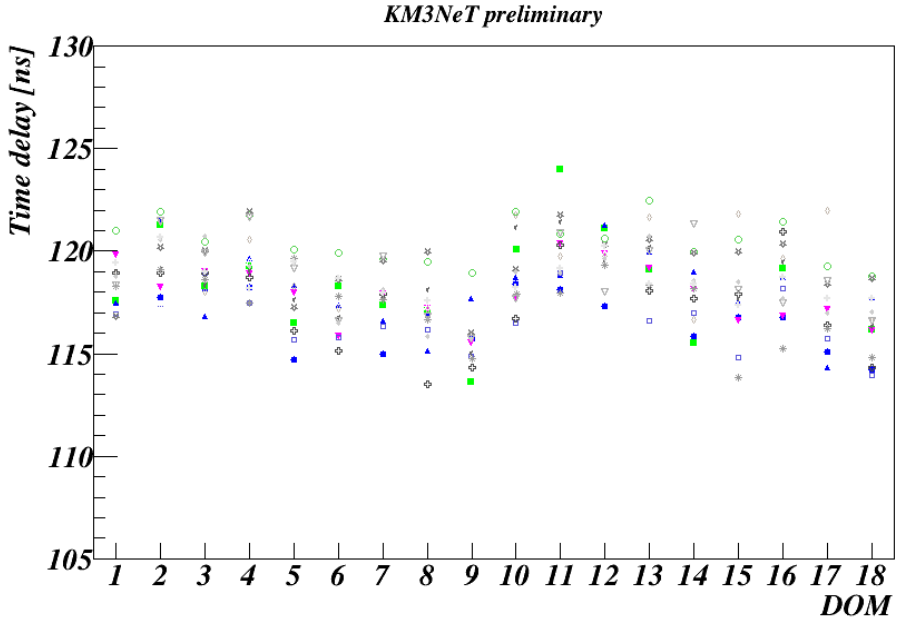

Figure 3: Mean value of arrival time distribution for top reference PMT, obtained by subtracting the laser pulse delay and the splitter delay. The data sample contains 15 DUs.

the GPS, are connected to two WWRSs (BM box) providing 2x1Gbps ethernet uplinks to shore. TriDAS and CU processes are also depicted in the picture. A light pulse generation at a wavelength of 406 nm is synchronized with a PPS signal from the DRY-WR, and the output feeds a path of fibers illuminating 36 PMTs through a 1/40 optical splitter, one on each DOM. The light signals are time stamped with respect to the reconstructed clock signal with the WR protocol. A few preliminary steps are needed: the time delay measurements of the light pulse at the laser output with respect to PPS signal, the delay of the splitter and the fine tuning of the light beam.

In Fig. 2 the arrival times of first light signals (collected from 1 PE hits) are shown: the time offset for the DOM is evaluated as the mean of a Gaussian fit to this distribution. Since the DOM readout electronics are segmented into two hemispheres, two PMTs of each DOM (one located in the upper and the other one in the lower hemisphere) are used for time calibration. These double-time measurements for each DOM allow for an essential redundancy in case of an issue of one PMT or readout electronics. In Fig. 3 and Fig. 4 the mean laser hit times are shown for all the DOM (top and bottom PMT reference) with the laser pulse and splitter delays subtracted. These measurements were performed on 15 DUs between February 2024 and May 2025 at Capacity laboratory. As can be seen from the two plots, all the DOMs are synchronized within a few ns exploiting the WR performance. These time offsets are used to correct and calibrate the timing of optical data from all DOMs. The residual time spread between DUs can be due to the different TTs (about ±2 ns), which we correct for in the water by the ^{40}K calibration and also by atmospheric muons. A modulo-9 effect can be also observed in the two plots. It is a systematic behaviour due to the different delay lines of connected DOMs for which ports the input/output delay corrections have not yet been applied. In Fig. 5 the offset comparison between the upper and lower hemispheres of the DOMs is shown. A time difference of about 1 ns is observed which can be explained by different electro-optic signal

PoS(ICRC2025)1116

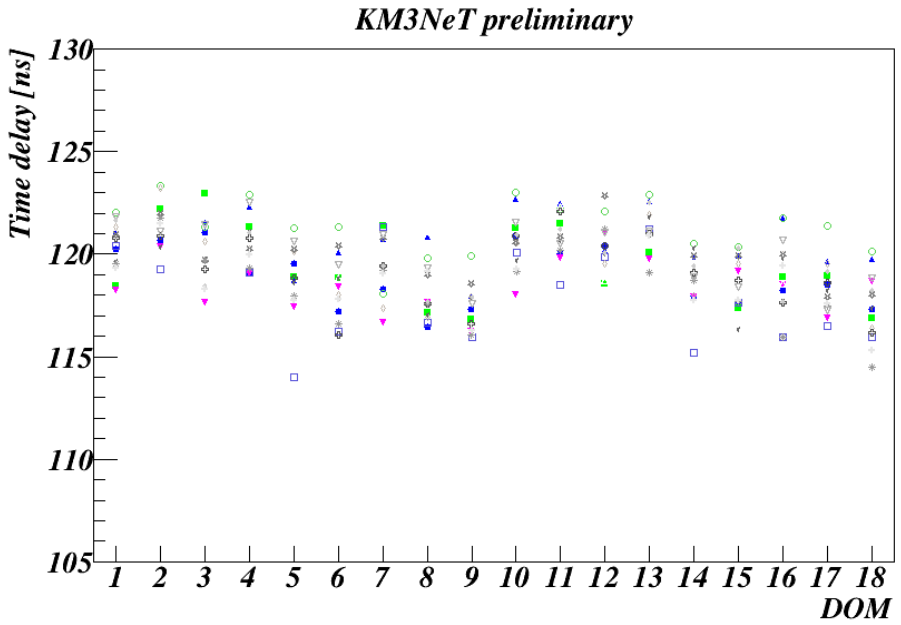

Figure 4: Mean value of arrival time distribution for bottom reference PMT, obtained by subtracting he laser pulse delay and the splitter delay. The data sample contains 15 DUs.

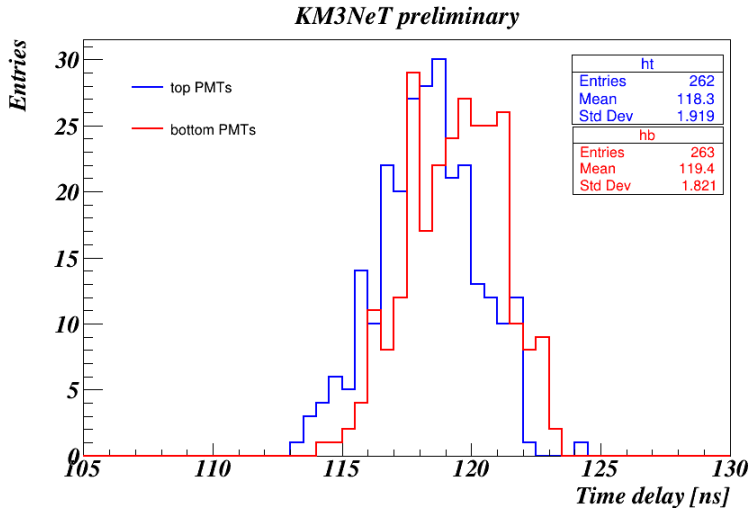

Figure 5: Distribution of the mean time values for top (blue) and bottom (red) reference PMT

processing.

The last part of the DU time measurements is devoted to the inter-DOM calibration by using a different configuration for WWRSA/B, namely backup link and redundant DOM configurations. In fact, the WWRS architecture allows for the use of an interlink (backup link) between WWRSA and WWRSB. Then, the laser runs are taken with different switch configurations.

PoS(ICRC2025)1116

3.6 Other checks

A crosscheck of the time offset calibration performed in the dark box can be carried out *in situ* after the DU deployment through the light emission diode beacon (Nanobeacon, NB) installed in the upper part of each DOM. A short light pulse at a fixed wavelength of 470 nm with the possibility to configure the intensity and frequency of flashing is controlled by the CLB logic. Measurement of time differences between pairs of DOMs allows calibration of the surrounding DOMs with respect to the one emitting light. Several runs with different bias voltages for the NB are acquired during DU calibration in order to evaluate the best operating voltage.

4. Conclusions

The ARCA DU calibration, as part of the integration process, has been described together with the test facility which includes on-shore/off-shore elements, network connections, timing synchronization components, and DAQ system to validate the detection unit under real operating conditions.
The procedures developed for the DU calibration are now applied to dozens of detection lines, part of which is deployed and operating under the sea. The calibration and quality control before the deployments shortens the detector comissioning after each deployment campaign.

References

[1] S. Adrián-Martínez, *et al.* (KM3NeT Collaboration), "Letter of intent for KM3NeT 2.0," *Journal of Physics G Nuclear Physics*, vol. 43, no. 8, p. 084001, Aug. 2016.

[2] S. Aiello, *et al.* (KM3NeT Collaboration), "The KM3NeT multi-PMT optical module," *Journal of Instrumentation*, vol. 17, no. 7, p. P07038, Jul. 2022.

[3] S. Aiello, *et al.* (KM3NeT Collaboration), "KM3NeT broadcast optical data transport system", JINST 18 T02001, 2023

[4] [Online]. Available:https://ohwr.org/project/white-rabbit.git. Accessed on June 13, 2019.

[5] S. Mastroianni et al., "Calibration Facility for Detector Strings for the KM3NeT/ARCA Neutrino Telescope at the Capacity Laboratory,", *IEEE TNS*, vol. 70, no. 6, pp. 1117-1123

[6] B. Jung, M. D. Jong, and P. Fermani, "PMT gain calibration and monitoring based on highly compressed hit information in KM3NeT," J. Instrum., vol. 16, no. 9, Sep. 2021

[7] G. Riccobene et al., "The KM3NeT-ARCA: Status and results of the Acoustic Positioning system", These Proceedings.

[8] F. Benfenati et al., "The White Rabbit Time Calibration system for KM3NeT-ARCA", These Proceedings.

PoS(ICRC2025)1116

Full Authors List: The KM3NeT Collaboration

O. Adriani [b,a], A. Albert[c,be], A.R. Alhebsi [d], S. Alshalloudi[d], M. Alshamsi[e], S. Alves Garre [f], F. Ameli[g], M. Andre[h], L. Aphecetche [i], M. Ardid [j], S. Ardid [j], J. Aublin[k], F. Badaracco [m,l], L. Bailly-Salins[n], B. Baret[k], A. Bariego-Quintana [f], M. Barnard [o], Y. Becherini[k], M. Bendahman[p], F. Benfenati Gualandi[r,q], M. Benhassi[s,p], D.M. Benoit [t], Z. Beňušová [v,u], E. Berbee[w], E. Berti[b], V. Bertin [e], P. Betti[b], S. Biagi [x], M. Boettcher[o], D. Bonanno [x], M. Bondì[y], S. Bottai[b], A.B. Bouasla[bf], J. Boumaaza[z], M. Bouta[e], M. Bouwhuis[w], C. Bozza [aa,p], R.M. Bozza[ab,p], H. Brânzaş[ac], F. Bretaudeau[i], M. Breuhaus [e], R. Bruijn[ad,w], J. Brunner[e], R. Bruno [y], E. Buis[w,ae], R. Buompane[s,p], I. Burriel[f], J. Busto[e], B. Caiffi[m], D. Calvo[f], A. Capone[g,af], F. Carenini[r,q], V. Carretero [ad,w], T. Cartraud[k], P. Castaldi[ag,q], V. Cecchini [f], S. Celli[g,af], L. Cerisy[e], M. Chabab[ah], A. Chen [ai], S. Cherubini[aj,x], T. Chiarusi[q], W. Chung[ak], M. Circella [al], R. Clark[am], R. Cocimano[x], J.A.B. Coelho[k], A. Coleiro[k], A. Condorelli[k], R. Coniglione[x], P. Coyle[e], A. Creusot[k], G. Cuttone[x], R. Dallier [i], A. De Benedittis[s,p], G. De Wasseige[am], V. Decoene[i], P. Deguire[e], I. Del Rosso[r,q], L.S. Di Mauro[x], I. Di Palma[g,af], A.F. Díaz[an], D. Diego-Tortosa [x], C. Distefano [x], A. Domi[ao], C. Donzaud[k], D. Dornic [e], E. Drakopoulou [ap], D. Drouhin [c,be], J.-G. Ducoin[e], P. Duverne[k], R. Dvornický [v], T. Eberl [ao], E. Eckerová[v,u], A. Eddymaoui[z], T. van Eeden[w], M. Eff[k], D. van Eijk[w], I. El Bojaddaini[aq], S. El Hedri[k], S. El Mentawi[e], V. Ellajosyula[m], A. Enzenhöfer[e], M. Farino[ak], G. Ferrara[aj,x], M.D. Filipović [ar], F. Filippini[q], D. Franciotti[x], L.A. Fusco[aa,p], T. Gal [ao], J. García Méndez [j], A. Garcia Soto [f], C. Gatius Oliver [w], N. Geißelbrecht[ao], E. Genton[am], H. Ghaddari[aq], L. Gialanella[s,p], B.K. Gibson[t], E. Giorgio[x], I. Goos [k], P. Goswami[k], S.R. Gozzini [f], R. Gracia[ao], B. Guillon[n], C. Haack[ao], C. Hanna[ak], H. van Haren[as], E. Hazelton[ak], A. Heijboer[w], L. Hennig[ao], J.J. Hernández-Rey[f], A. Idrissi [x], W. Idrissi Ibnsalih[p], G. Illuminati[q], R. Jaimes[f], O. Janik[ao], D. Joly[e], M. de Jong[at,w], P. de Jong[ad,w], B.J. Jung[w], P. Kalaczyński [bg,au], U.F. Katz[ao], J. Keegans[t], V. Kikvadze[av], G. Kistauri[aw,av], C. Kopper [ao], A. Kouchner[ax,k], Y.Y. Kovalev [ay], L. Krupa[u], V. Kueviakoe[w], V. Kulikovskiy[m], R. Kvatadze[aw], M. Labalme[n], R. Lahmann[ao], M. Lamoureux [am], A. Langella [ak], G. Larosa[x], C. Lastoria[n], J. Lazar[am], A. Lazo[f], G. Lehaut[n], V. Lemaître[am], E. Leonora[y], N. Lessing[f], G. Levi[r,q], M. Lindsey Clark[k], F. Longhitano[y], S. Madarapu[f], F. Magnani[e], L. Malerba[m,l], F. Mamedov[u], A. Manfreda [p], A. Manousakis[az], M. Marconi [l,m], A. Margiotta [r,q], A. Marinelli[ab,p], C. Markou[ap], L. Martin [i], M. Mastrodicasa[af,g], S. Mastroianni[p], J. Mauro [am], K.C.K. Mehta[au], G. Miele[ab,p], P. Migliozzi [p], E. Migneco[x], M.L. Mitsou[s,p], C.M. Mollo[p], L. Morales-Gallegos [s,p], N. Mori [b], A. Moussa [aq], I. Mozun Mateo[n], R. Muller [q], M.R. Musone[s,p], M. Musumeci[x], S. Navas [ba], A. Nayerhoda[al], C.A. Nicolau[g], B. Nkosi [ai], B. Ó Fearraigh [m], V. Oliviero [ab,p], A. Orlando[x], E. Oukacha[k], L. Pacini [b], D. Paesani[x], J. Palacios González [f], G. Papalashvili[al,av], P. Papini[b], V. Parisi[l,m], A. Parmar[n], C. Pastore[al], A.M. Păun[ac], G.E. Păvălaş[ac], S. Peña Martínez [k], M. Perrin-Terrin[e], V. Pestel[n], M. Petropavlova [u,bh], P. Piattelli[x], A. Plavin[ay,bi], C. Poirè[aa,p], V. Popa[†2,ac], T. Pradier [c], J. Prado[f], S. Pulvirenti[x], C.A. Quiroz-Rangel [j], N. Randazzo[y], A. Ratnani[bb], S. Razzaque[bc], I.C. Rea [p], D. Real [f], G. Riccobene [x], J. Robinson[o], A. Romanov[l,m,n], E. Ros[ay], A. Šaina[f], F. Salesa Greus [f], D.F.E. Samtleben[at,w], A. Sánchez Losa [f], S. Sanfilippo[x], M. Sanguineti[l,m], D. Santonocito[x], P. Sapienza[x], M. Scaringella[b], M. Scarnera[am,k], J. Schnabel[ao], J. Schumann [ao], J. Seneca[w], P.A. Sevle Myhr [am], I. Sgura[al], R. Shanidze[av], Chengyu Shao [bj,e], A. Sharma[k], Y. Shitov[u], F. Šimkovic[v], A. Simonelli[p], A. Sinopoulou [y], B. Spisso[p], M. Spurio [r,q], O. Starodubtsev[b], D. Stavropoulos[ap], I. Štekl[u], D. Stocco [i], M. Taiuti[l,m], Y. Tayalati[z,bb], H. Thiersen[o], I. Tosta e Melo[y,aj], B. Trocmé [k], V. Tsourapis [ap], C. Tully [ak], E. Tzamariudaki[ap], A. Ukleja [au], A. Vacheret[n], V. Valsecchi[x], V. Van Elewyck[ax,k], G. Vannoye[l,m], E. Vannuccini[b], G. Vasileiadis[bd], F. Vazquez de Sola[w], A. Veutro[g,af], S. Viola[x], D. Vivolo[s,p], A. van Vliet [d], E. de Wolf [ad,w], I. Lhenry-Yvon[k], S. Zavatarelli[m], D. Zito[x], J.D. Zornoza [f], and J. Zúñiga [f].

[a] Università di Firenze, Dipartimento di Fisica e Astronomia, via Sansone 1, Sesto Fiorentino, 50019 Italy
[b] INFN, Sezione di Firenze, via Sansone 1, Sesto Fiorentino, 50019 Italy
[c] Université de Strasbourg, CNRS, IPHC UMR 7178, F-67000 Strasbourg, France
[d] Khalifa University of Science and Technology, Department of Physics, PO Box 127788, Abu Dhabi, United Arab Emirates
[e] Aix Marseille Univ, CNRS/IN2P3, CPPM, Marseille, France
[f] IFIC - Instituto de Física Corpuscular (CSIC - Universitat de València), c/Catedrático José Beltrán, 2, 46980 Paterna, Valencia, Spain
[g] INFN, Sezione di Roma, Piazzale Aldo Moro, 2 - c/o Dipartimento di Fisica, Edificio, G.Marconi, Roma, 00185 Italy
[h] Universitat Politècnica de Catalunya, Laboratori d'Aplicacions Bioacústiques, Centre Tecnològic de Vilanova i la Geltrú, Avda. Rambla Exposició, s/n, Vilanova i la Geltrú, 08800 Spain
[i] Subatech, IMT Atlantique, IN2P3-CNRS, Nantes Université, 4 rue Alfred Kastler - La Chantrerie, Nantes, BP 20722 44307 France
[j] Universitat Politècnica de València, Instituto de Investigación para la Gestión Integrada de las Zonas Costeras, C/ Paranimf, 1, Gandia, 46730 Spain
[k] Université Paris Cité, CNRS, Astroparticule et Cosmologie, F-75013 Paris, France
[l] Università di Genova, Via Dodecaneso 33, Genova, 16146 Italy
[m] INFN, Sezione di Genova, Via Dodecaneso 33, Genova, 16146 Italy
[n] LPC CAEN, Normandie Univ, ENSICAEN, UNICAEN, CNRS/IN2P3, 6 boulevard Maréchal Juin, Caen, 14050 France
[o] North-West University, Centre for Space Research, Private Bag X6001, Potchefstroom, 2520 South Africa
[p] INFN, Sezione di Napoli, Complesso Universitario di Monte S. Angelo, Via Cintia ed. G, Napoli, 80126 Italy
[q] INFN, Sezione di Bologna, v.le C. Berti-Pichat, 6/2, Bologna, 40127 Italy
[r] Università di Bologna, Dipartimento di Fisica e Astronomia, v.le C. Berti-Pichat, 6/2, Bologna, 40127 Italy

[2] Deceased

PoS(ICRC2025)1116

[s] Università degli Studi della Campania "Luigi Vanvitelli", Dipartimento di Matematica e Fisica, viale Lincoln 5, Caserta, 81100 Italy
[t] E. A. Milne Centre for Astrophysics, University of Hull, Hull, HU6 7RX, United Kingdom
[u] Czech Technical University in Prague, Institute of Experimental and Applied Physics, Husova 240/5, Prague, 110 00 Czech Republic
[v] Comenius University in Bratislava, Department of Nuclear Physics and Biophysics, Mlynska dolina F1, Bratislava, 842 48 Slovak Republic
[w] Nikhef, National Institute for Subatomic Physics, PO Box 41882, Amsterdam, 1009 DB Netherlands
[x] INFN, Laboratori Nazionali del Sud, (LNS) Via S. Sofia 62, Catania, 95123 Italy
[y] INFN, Sezione di Catania, (INFN-CT) Via Santa Sofia 64, Catania, 95123 Italy
[z] University Mohammed V in Rabat, Faculty of Sciences, 4 av. Ibn Battouta, B.P. 1014, R.P. 10000 Rabat, Morocco
[aa] Università di Salerno e INFN Gruppo Collegato di Salerno, Dipartimento di Fisica, Via Giovanni Paolo II 132, Fisciano, 84084 Italy
[ab] Università di Napoli "Federico II", Dip. Scienze Fisiche "E. Pancini", Complesso Universitario di Monte S. Angelo, Via Cintia ed. G, Napoli, 80126 Italy
[ac] Institute of Space Science - INFLPR Subsidiary, 409 Atomistilor Street, Magurele, Ilfov, 077125 Romania
[ad] University of Amsterdam, Institute of Physics/IHEF, PO Box 94216, Amsterdam, 1090 GE Netherlands
[ae] TNO, Technical Sciences, PO Box 155, Delft, 2600 AD Netherlands
[af] Università La Sapienza, Dipartimento di Fisica, Piazzale Aldo Moro 2, Roma, 00185 Italy
[ag] Università di Bologna, Dipartimento di Ingegneria dell'Energia Elettrica e dell'Informazione "Guglielmo Marconi", Via dell'Università 50, Cesena, 47521 Italia
[ah] Cadi Ayyad University, Physics Department, Faculty of Science Semlalia, Av. My Abdellah, P.O.B. 2390, Marrakech, 40000 Morocco
[ai] University of the Witwatersrand, School of Physics, Private Bag 3, Johannesburg, Wits 2050 South Africa
[aj] Università di Catania, Dipartimento di Fisica e Astronomia "Ettore Majorana", (INFN-CT) Via Santa Sofia 64, Catania, 95123 Italy
[ak] Princeton University, Department of Physics, Jadwin Hall, Princeton, New Jersey, 08544 USA
[al] INFN, Sezione di Bari, via Orabona, 4, Bari, 70125 Italy
[am] UCLouvain, Centre for Cosmology, Particle Physics and Phenomenology, Chemin du Cyclotron, 2, Louvain-la-Neuve, 1348 Belgium
[an] University of Granada, Department of Computer Engineering, Automation and Robotics / CITIC, 18071 Granada, Spain
[ao] Friedrich-Alexander-Universität Erlangen-Nürnberg (FAU), Erlangen Centre for Astroparticle Physics, Nikolaus-Fiebiger-Straße 2, 91058 Erlangen, Germany
[ap] NCSR Demokritos, Institute of Nuclear and Particle Physics, Ag. Paraskevi Attikis, Athens, 15310 Greece
[aq] University Mohammed I, Faculty of Sciences, BV Mohammed VI, B.P. 717, R.P. 60000 Oujda, Morocco
[ar] Western Sydney University, School of Science, Locked Bag 1797, Penrith, NSW 2751 Australia
[as] NIOZ (Royal Netherlands Institute for Sea Research), PO Box 59, Den Burg, Texel, 1790 AB, the Netherlands
[at] Leiden University, Leiden Institute of Physics, PO Box 9504, Leiden, 2300 RA Netherlands
[au] AGH University of Krakow, Al. Mickiewicza 30, 30-059 Krakow, Poland
[av] Tbilisi State University, Department of Physics, 3, Chavchavadze Ave., Tbilisi, 0179 Georgia
[aw] The University of Georgia, Institute of Physics, Kostava str. 77, Tbilisi, 0171 Georgia
[ax] Institut Universitaire de France, 1 rue Descartes, Paris, 75005 France
[ay] Max-Planck-Institut für Radioastronomie, Auf dem Hügel 69, 53121 Bonn, Germany
[az] University of Sharjah, Sharjah Academy for Astronomy, Space Sciences, and Technology, University Campus - POB 27272, Sharjah, - United Arab Emirates
[ba] University of Granada, Dpto. de Física Teórica y del Cosmos & C.A.F.P.E., 18071 Granada, Spain
[bb] School of Applied and Engineering Physics, Mohammed VI Polytechnic University, Ben Guerir, 43150, Morocco
[bc] University of Johannesburg, Department Physics, PO Box 524, Auckland Park, 2006 South Africa
[bd] Laboratoire Univers et Particules de Montpellier, Place Eugène Bataillon - CC 72, Montpellier Cédex 05, 34095 France
[be] Université de Haute Alsace, rue des Frères Lumière, 68093 Mulhouse Cedex, France
[bf] Université Badji Mokhtar, Département de Physique, Faculté des Sciences, Laboratoire de Physique des Rayonnements, B. P. 12, Annaba, 23000 Algeria
[bg] AstroCeNT, Nicolaus Copernicus Astronomical Center, Polish Academy of Sciences, Rektorska 4, Warsaw, 00-614 Poland
[bh] Charles University, Faculty of Mathematics and Physics, Ovocný trh 5, Prague, 116 36 Czech Republic
[bi] Harvard University, Black Hole Initiative, 20 Garden Street, Cambridge, MA 02138 USA

Acknowledgements

The authors acknowledge the financial support of: KM3NeT-INFRADEV2 project, funded by the European Union Horizon Europe Research and Innovation Programme under grant agreement No 101079679; Funds for Scientific Research (FRS-FNRS), Francqui foundation, BAEF foundation. Czech Science Foundation (GAČR 24-12702S); Agence Nationale de la Recherche (contract ANR-15-CE31-0020), Centre National de la Recherche Scientifique (CNRS), Commission Européenne (FEDER fund and Marie Curie Program), LabEx UnivEarthS (ANR-10-LABX-0023 and ANR-18-IDEX-0001), Paris Île-de-France Region, Normandy Region (Alpha, Blue-waves and Neptune), France, The Provence-Alpes-Côte d'Azur Delegation for Research and Innovation (DRARI), the Provence-Alpes-Côte d'Azur region, the Bouches-du-Rhône Departmental Council, the Metropolis of Aix-Marseille Provence and the City of Marseille through the

PoS(ICRC2025)1116

CPER 2021-2027 NEUMED project, The CNRS Institut National de Physique Nucléaire et de Physique des Particules (IN2P3); Shota Rustaveli National Science Foundation of Georgia (SRNSFG, FR-22-13708), Georgia; This research was funded by the European Union (ERC MuSES project No 101142396); The General Secretariat of Research and Innovation (GSRI), Greece; Istituto Nazionale di Fisica Nucleare (INFN) and Ministero dell'Università e della Ricerca (MUR), through PRIN 2022 program (Grant PANTHEON 2022E2J4RK, Next Generation EU) and PON R&I program (Avviso n. 424 del 28 febbraio 2018, Progetto PACK-PIR01 00021), Italy; IDMAR project Po-Fesr Sicilian Region az. 1.5.1; A. De Benedittis, W. Idrissi Ibnsalih, M. Bendahman, A. Nayerhoda, G. Papalashvili, I. C. Rea, A. Simonelli have been supported by the Italian Ministero dell'Università e della Ricerca (MUR), Progetto CIR01 00021 (Avviso n. 2595 del 24 dicembre 2019); KM3NeT4RR MUR Project National Recovery and Resilience Plan (NRRP), Mission 4 Component 2 Investment 3.1, Funded by the European Union – NextGenerationEU,CUP I57G21000040001, Concession Decree MUR No. n. Prot. 123 del 21/06/2022; Ministry of Higher Education, Scientific Research and Innovation, Morocco, and the Arab Fund for Economic and Social Development, Kuwait; Nederlandse organisatie voor Wetenschappelijk Onderzoek (NWO), the Netherlands; The grant "AstroCeNT: Particle Astrophysics Science and Technology Centre", carried out within the International Research Agendas programme of the Foundation for Polish Science financed by the European Union under the European Regional Development Fund; The program: "Excellence initiative-research university" for the AGH University in Krakow; The ARTIQ project: UMO-2021/01/2/ST6/00004 and ARTIQ/0004/2021; Ministry of Education and Scientific Research, Romania; Slovak Research and Development Agency under Contract No. APVV-22-0413; Ministry of Education, Research, Development and Youth of the Slovak Republic; MCIN for PID2021-124591NB-C41, -C42, -C43 and PDC2023-145913-I00 funded by MCIN/AEI/10.13039/501100011033 and by "ERDF A way of making Europe", for ASFAE/2022/014 and ASFAE/2022 /023 with funding from the EU NextGenerationEU (PRTR-C17.I01) and Generalitat Valenciana, for Grant AST22_6.2 with funding from Consejería de Universidad, Investigación e Innovación and Gobierno de España and European Union - NextGenerationEU, for CSIC-INFRA23013 and for CNS2023-144099, Generalitat Valenciana for CIDEGENT/2020/049, CIDEGENT/2021/23, CIDEIG/2023/20, ESGENT2024/24, CIPROM/2023/51, GRISOLIAP/2021/192 and INNVA1/2024/110 (IVACE+i), Spain; Khalifa University internal grants (ESIG-2023-008, RIG-2023-070 and RIG-2024-047), United Arab Emirates; The European Union's Horizon 2020 Research and Innovation Programme (ChETEC-INFRA - Project no. 101008324).

Views and opinions expressed are those of the author(s) only and do not necessarily reflect those of the European Union or the European Research Council. Neither the European Union nor the granting authority can be held responsible for them.

PoS(ICRC2025)1116